

Mott lobes of the $S = 1$ Bose-Hubbard model with three-body interactions

A. F. Hincapié-F, R. Franco, and J. Silva-Valencia*

Departamento de Física, Universidad Nacional de Colombia, A. A. 5997 Bogotá, Colombia.

(Dated: March 19, 2019)

Using the density matrix renormalization group method, we studied the ground state of the one-dimensional $S = 1$ Bose-Hubbard model with local three-body interactions, which can be a superfluid or a Mott insulator state. We drew the phase diagram of this model for both ferromagnetic and antiferromagnetic interaction. Regardless of the sign of the spin-dependent coupling, we obtained that the Mott lobes area decreases as the spin-dependent strength increases, which means that the even-odd asymmetry of the two-body antiferromagnetic chain is absent for local three-body interactions. For antiferromagnetic coupling, we found that the density drives first-order superfluid-Mott insulator transitions for even and odd lobes. Ferromagnetic Mott insulator and superfluid states were obtained with a ferromagnetic coupling, and a tendency to a “long-range” order was observed.

I. INTRODUCTION

The use of the optical lattices as an emulator for condensed matter physics has opened the door to new developments with ultracold atoms [1], and the observation of a quantum phase transition from a superfluid to a Mott insulator state by Greiner *et al.* [2] using ^{87}Rb atoms increased the study of atoms confined in optical traps. This transition was predicted by Jaksch *et al.* [3] considering the spinless Bose-Hubbard Hamiltonian, which has been widely studied, and its phase diagram is well known [4–6].

The subsequent development of experimental techniques has allowed confining atoms in purely optical traps such that the degree of freedom of spin is not frozen, allowing the creation of spinor condensates, which exhibit new quantum physical properties, and this has stimulated the study of quantum magnetism with cold atom setups [7]. Alkali atoms such as ^{87}Rb or ^{23}Na have a nuclear spin $I = 3/2$ and an electronic spin $J = \pm 1/2$, so that these atoms can be confined with a hyperfine spin state 1 or 2. The effective Hamiltonian to describe the behavior of spin-1 bosons in optical lattices was proposed by Imambekov *et al.* [8, 9]. In order to obtain it, they considered two channels in the contact interaction. Therefore, the Hamiltonian contains a kinetic term and two local interaction terms, the two-body repulsion and a spin-dependent interaction. This model has been widely studied in one dimension by using mean-field approximations and numerical techniques, and its phase diagram is known [9–15]. There exist Mott insulator lobes and a superfluid region, among which quantum phase transitions occur. It has been shown that when the local spin interaction is antiferromagnetic, the system has an asymmetry in the Mott lobes: the even ones grow with an increase in the spin interaction parameter, while odd lobes decrease [8]. Also, within the odd lobes a competition between a dimerized and a nematic singlet phase has

been explored [11, 12, 16–18]. On the other hand, for ferromagnetic interaction the lobes always decrease as the spin interaction parameter increases, and the magnetic ordering within the lobes is “long-range” ferromagnetic order [14]. Furthermore, it has been shown that for antiferromagnetic interaction the phase transition is first-order for even lobes due to the coexistence of singlets in the two phases, while for odd ones it is a second-order transition [14].

Several authors have studied this model in two-dimensional lattices, showing that the system in the superfluid phase exhibits a nematic order and the phase transition from superfluid to Mott insulator is first or second order if the density at the Mott lobe is even or odd, respectively [18–20].

Recently, upon studying the dynamics of spin-1 bosons loaded in a 3D optical lattice, Mahmud *et al.* showed that the Hamiltonian to describe the physics of the system does not contain only two-body interactions: multi-body interactions make the model more accurate. Also, by means of the perturbation theory they derived an effective spin-dependent and spin-independent three-body interaction terms [21].

For spinless bosons systems, local and non-local multi-body interaction terms have been considered during the last decade. For instance, Büchler *et al.* [22] proposed that polar molecules in optical lattices can be tuned to a regime where three-body interactions play the dominant role, and Jhonson *et al.* [23] obtained that two-body interactions generate effective higher-body interactions. Also, in 2010 Will *et al.* [24] showed experimental evidence of multi-body interactions using an interferometric technique for ^{87}Rb atoms confined in an optical lattice, and after that, resonances were associated with higher-order processes in photon-assisted tunneling experiments [25]. Other authors have stated that when considering complex geometries like the double-well optical lattice, the effective Hamiltonian contains strong three-body interactions tuned by lattice parameters [26]. On the other hand, Daley *et al.* [27] proposed an experimental setup using laser-assisted tunneling in a bosonic gas in which the three-body interactions dominate the physics

* jsilvav@unal.edu.co

of the system. Very recently, using Feshbach resonance, a novel way to get rid of the two-body interactions has been proposed. This interaction strength can be obtained as a function of the scattering length and an effective range. These two can be tuned until the two-body interaction term vanishes while three atoms interact at the same lattice site via three-body contact repulsion [28].

Phase diagrams of spinless bosons under three-body interactions in one dimension have been studied and found by several authors. For instance, bosons under on-site interactions [29–32], nearest neighbor interaction [33], and contact three body interaction [34] have been considered. An interesting result obtained for the on-site case was that the area of the first Mott lobe (two bosons per site) decreases while the second Mott lobe grows as the three-body strength increases.

Taking into account that the physics of spinor bosons in one dimension is very interesting and the fact that multi-body interactions can generate new phases and the perturbative calculation of the three-body local interaction terms between spin-1 bosons, in the present paper we explore a one-dimensional system of spinor bosons that interact under local three-body terms. To our knowledge, this problem has not been studied, and we calculate the ground state energy and the correlation functions by using the density matrix renormalization group method for ferromagnetic and antiferromagnetic interactions. For both kinds of interactions, we found that the phase diagram has Mott insulator lobes and a superfluid region. We obtained that the area of the Mott insulator lobes decreases with the spin-dependent term, and also a quantum phase transition in the superfluid region was found.

The structure of the paper is as follows: In Sec. II we explain the Hamiltonian of the $S = 1$ Bose-Hubbard model with three-body interaction. In Sec. III we show the evolution of the chemical potential and the correlation functions as a function of the system parameters for antiferromagnetic and ferromagnetic spin-dependent interaction; finding diverse phase diagrams for both cases. The last section, Sec. IV, contains a summary and conclusions.

II. MODEL

In 2013, Mahmud and Tiesinga made a perturbative calculation and found the effective expressions for the interaction among three spin-1 bosons. These expressions are local and are given in terms of the density and spin operators [21]. The Hamiltonian of the unexplored problem of one-dimensional spinor bosons interacting through

only three-body terms is given by

$$\begin{aligned} \mathcal{H} = & -t \sum_{i,\sigma} \left(b_{i,\sigma}^\dagger b_{i+1,\sigma} + \text{h.c.} \right) \\ & + \frac{V_0}{6} \sum_i \hat{n}_i (\hat{n}_i - 1) (\hat{n}_i - 2) \\ & + \frac{V_2}{6} \sum_i (\hat{\mathbf{S}}_i^2 - 2\hat{n}_i) (\hat{n}_i - 2), \end{aligned} \quad (1)$$

where $b_{i,\sigma}^\dagger (b_{i,\sigma})$ creates (annihilates) a boson with spin component σ on site i of a one-dimensional optical lattice of size L , $\hat{n}_i = \sum_\sigma b_{i,\sigma}^\dagger b_{i,\sigma}$ and $\hat{\mathbf{S}}_i = \sum_{\sigma,\sigma'} b_{i,\sigma}^\dagger \mathbf{T}_{\sigma,\sigma'} b_{i,\sigma'}$ are the total number of particles and the spin operators on site i , respectively. $\mathbf{T}_{\sigma,\sigma'}$ are the spin-1 Pauli matrices.

The first term in the Hamiltonian (1) is the kinetic energy modulated by t , which is a measure of the tunneling force between nearest sites. The second term represents the short-range interaction between three or more atoms at the same site, where V_0 is the on-site repulsion parameter. The last term in the Hamiltonian is the local spin exchange interaction, tuned by the V_2 parameter. The latter can be positive or negative, according to the nature of the interaction, ferromagnetic (^{87}Rb) or antiferromagnetic (^{23}Na), respectively. For a harmonic potential with frequency ω_f , V_0 is given by $V_0 = -1.34 \frac{U_0^2}{(\hbar\omega_f)}$ and V_2 is given by $V_2 = 2 \frac{U_2}{U_0} V_0$ [23], where U_0 and U_2 are the two-body strengths parameters given by $U_0 = 4\pi\hbar^2(a_0 + 2a_2)/3M$ and $U_2 = 4\pi\hbar^2(a_2 - a_0)/3M$, where a_s are the scattering lengths for $S = 0$ and $S = 2$ channels, and M is the mass of the atom [35]. The fraction $\frac{U_2}{U_0}$ can be determined from experimental scattering lengths, and it is 0.04 for ^{23}Na and -0.01 for ^{87}Rb [36, 37].

Note that for spinless bosons interacting through three-body on-site terms, the phase diagram exhibits Mott insulator regions, and a superfluid phase surrounding them. However, in order to obtain a Mott insulator state, we need at least two bosons per site [30, 31]. When we consider spinor bosons, it is expected that insulator and superfluid phases will appear, and the border that separates these phases can be estimated by means of the energy gap for adding or removing one particle from the system, taking into account the canonical ensemble. This gap is given by $\Delta(L) = \mu^p(L) - \mu^h(L)$ where the chemical potential for adding or removing a particle is given by

$$\mu^p(L) = E_0(L, S_{tot}^z, N+1) - E_0(L, S_{tot}^z, N),$$

$$\mu^h(L) = E_0(L, S_{tot}^z, N) - E_0(L, S_{tot}^z, N-1).$$

$E_0(L, S_{tot}^z, N)$ being the ground state energy for L sites, N particles with S_{tot}^z the z -component of the total spin.

III. RESULTS

In order to determine the phase diagram of the Hamiltonian (1), we employed the density matrix renormaliza-

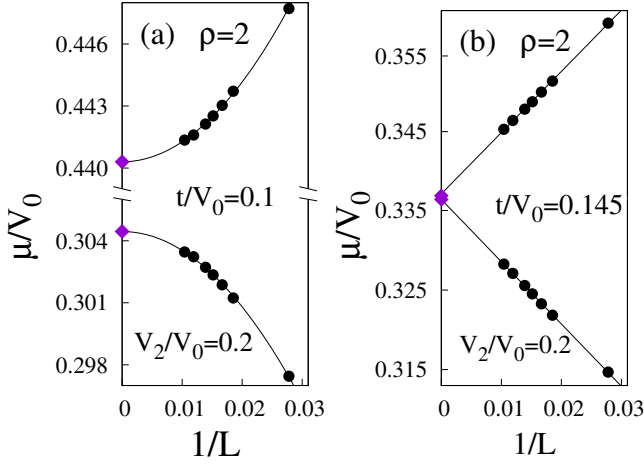


FIG. 1. System size dependence on the chemical potential at $\rho = 2$ and $V_2/V_0 = 0.2$. The left panel shows a gapped state with an integer number of particles per site for $t/V_0 = 0.1$, and in the right panel the system is in a gapless state for $t/V_0 = 0.145$. The upper set of data corresponds to the energy for adding a particle, and the lower one to the energy for removing one. The values at the thermodynamic limit (diamonds) were obtained by fitting the DMRG results (circles) in the left (right) panel to the function $\mu^{p,h}(L) = \tilde{\mu}^{p,h} + c_1/L + c_2/L^2$ ($\mu^{p,h}(L) = \tilde{\mu}^{p,h} + c_3/L$), where c_i are constants. The lines are visual guides

tion group (DMRG) method with open boundary conditions [38]. We used the finite-size algorithm for sizes up to $L = 96$ unless otherwise written. Fixing the parameters of our problem, we calculated the energy for different values of the total spin along z ($S_{tot}^z = 0, 1$ and 2) and we obtained that the ground state is degenerate, which suggests that the Katsura theorems are valid for this model, and therefore all calculations presented in this paper are in the sector with spin component $S_{tot}^z = 0$ in order to determine the ground-state energy [39]. The dimension of the local Hilbert space basis is fixed by choosing a maximum occupation number \hat{n}_{max} . We chose $\hat{n}_{max} = 5$ in order to guarantee accurate results, keeping up to $m = 300$ states per block, and obtained a discarded weight around 10^{-5} or less. We set our energy scale choosing $V_0 = 1$ and explored the phase diagram by changing the parameter V_2 .

A. Antiferromagnetic case ($V_2 > 0$)

First of all, we analyze the system in the non-hopping case $t \rightarrow 0$, the atomic limit. For n_i particles, the energy is given by

$$E_M(n_i) = \frac{V_0}{6} n_i(n_i - 1)(n_i - 2) + \frac{V_2}{6} [\langle \hat{S}_i^2 \rangle - 2n_i] (n_i - 2).$$

For the antiferromagnetic case, we need to separate the analysis for even and odd densities. The expectation

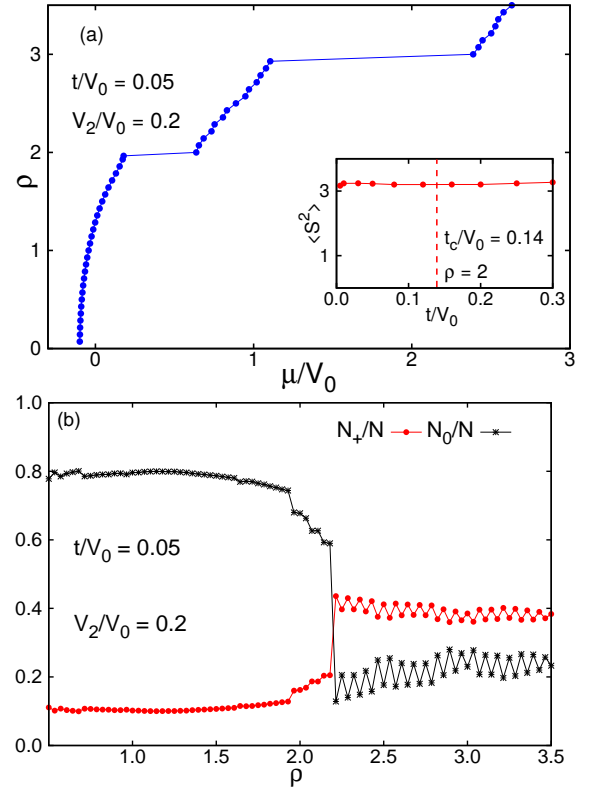


FIG. 2. (a) The global particle density ρ as a function of the chemical potential μ exhibits a Mott insulator plateau at integer densities greater than one. The inset shows the evolution of $\langle S^2 \rangle$ as a function of the hopping parameter t/V_0 for a density $\rho = 2$. The vertical dashed line indicates the position of the Mott insulator-superfluid transition. (b) The spin population fractions N_+/N and N_0/N as a function of the global density ρ for $t/V_0 = 0.05$, $V_2/V_0 = 0.2$, and $L = 28$.

value $\langle \hat{S}_i^2 \rangle = S(S+1)$ has an important role at this point: if the system has an even filling, it could have a ground state composed of singlets at each site ($S = 0 \rightarrow \langle \hat{S}_i^2 \rangle = 0$), whereas for odd filling there will always be an unpaired boson at each site ($S = 1 \rightarrow \langle \hat{S}_i^2 \rangle = 2$). So for even filling, n_e , the energy of the Mott lobes is $E_M(n_e) = V_0 n_e(n_e - 1)(n_e - 2)/6 - V_2 n_e(n_e - 2)/3$, while for odd filling, n_o , $E_M(n_o) = V_0 n_o(n_o - 1)(n_o - 2)/6 + V_2(1 - n_o)(n_o - 2)/3$. Thus the boundaries of the Mott lobes can be determined from the energy difference $\mu_0(n \rightarrow n+1) = E_M(n+1) - E_M(n)$ between the Mott ground state with n and with $n+1$ particles (here μ_0 represents the chemical potential at $t = 0$). Taking into account the above definition, we obtain $\mu_0(n_e \rightarrow n_{e+1}) = n_e(n_e - 1)V_0/2 - n_e V_2/3$ and $\mu_0(n_o \rightarrow n_{o+1}) = n_o(n_o - 1)V_0/2 - (n_o - 1)V_2$.

We can see that the borders of the Mott lobes decrease due to the spin interaction, regardless of the global density, in contrast with the model with two-body interactions, for which the upper border of the second Mott lobe

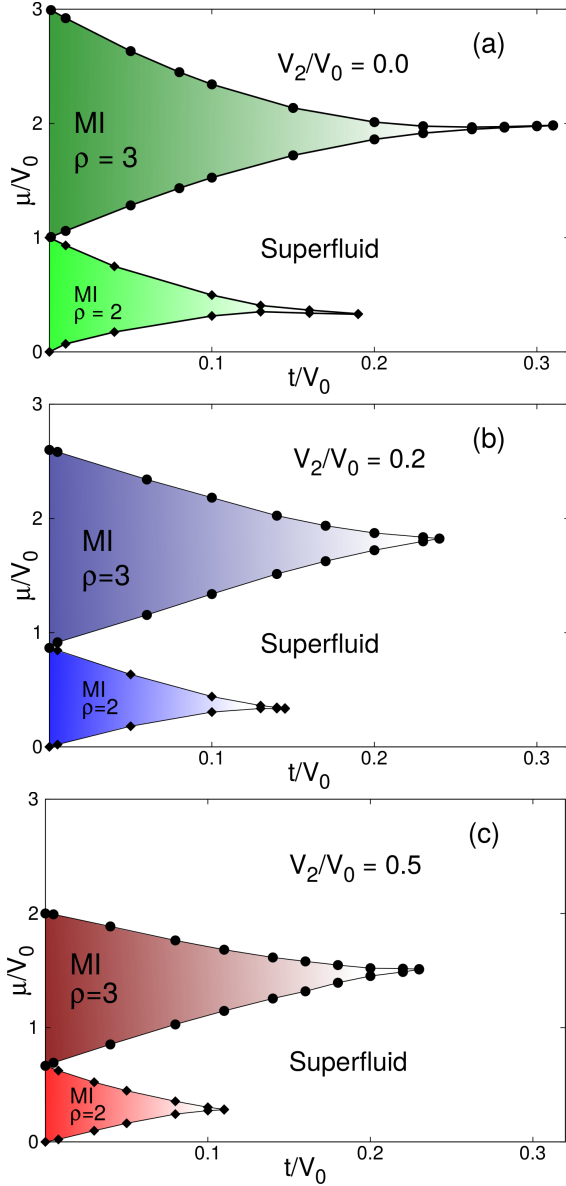


FIG. 3. Phase diagram for the first two Mott lobes of the spin-1 Bose-Hubbard model with three-body interaction and antiferromagnetic spin interaction. (a) $V_2/V_0 = 0$, (b) $V_2/V_0 = 0.2$, and (c) $V_2/V_0 = 0.5$. The solid lines are visual guides.

remains fixed at $\mu_0/U_0 = 2$. Therefore, for spinor bosons interacting with three-body terms, we obtain that at the atomic limit the upper border of the first (second) Mott lobe is given by $\mu_0^*/V_0 = 1 - \frac{2V_2}{3V_0}$ ($\mu_0^*/V_0 = 3 - 2\frac{V_2}{V_0}$).

The behavior of the chemical potential with respect to the system size is shown in Fig. 1 for global density $\rho = N/L = 2$ and $V_2/V_0 = 0.2$. In the left panel (Fig. 1a), we consider $t/V_0 = 0.1$ and see that the energy for adding (removing) a particle decreases (increases), following a quadratic behavior, as the lattice size increases. It is possible to determine that the value of the energy gap at the thermodynamic limit ($N, L \rightarrow \infty$) is finite

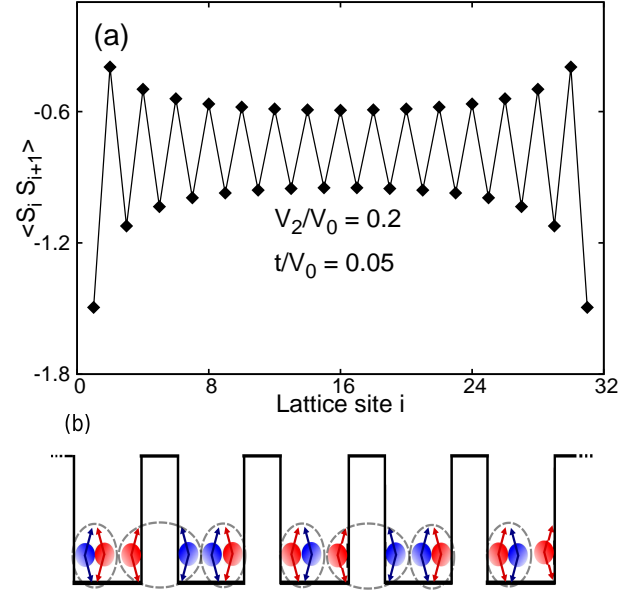


FIG. 4. (a) Spin-spin correlations for a spinor boson chain with antiferromagnetic spin-dependent interaction. The parameters used are $\rho = 3$, $L = 32$, and $t/V_0 = 0.05$, which correspond to the second Mott insulator lobe. (b) Schematic of a possible microscopic configuration for the dimerized Mott state for $\rho = 3$.

and not zero $\Delta/V_0 = 0.136$, and due to the integer number of atoms at each lattice site, the system is in a Mott insulator state. Increasing the hopping parameter to $t/V_0 = 0.145$, we observe that the energy for adding (removing) a particle decreases (increases), following a linear behavior, as the lattice size increases, and at the thermodynamic limit the value is the same, i. e. the gap vanishes and the system is in a superfluid state (Fig. 1b). We stated based on Fig. 1 that the system undergoes a quantum phase transition as the kinetic energy of the bosons increases.

Varying the number of particles and calculating the ground-state energy for each set of parameters with a fixed lattice size, we can determine the behavior of the chemical potential as a function of the global density, which is shown in Fig. 2a for a spinor chain with antiferromagnetic spin-dependent interaction $V_2/V_0 = 0.2$ and a hopping parameter $t/V_0 = 0.05$. We observe that as the global density increases, the chemical potential increases monotonously, passing through the value $\rho = 1$ without major changes, which indicates that the Hamiltonian (1) does not exhibit a Mott insulator state for a filling of one atom per site, a result that is well known for the model with two-body interactions. This happens because the quantum fluctuations are not large enough to generate a Mott insulator state with three-body local interactions. The continuous growth of the chemical potential as a function of the global density ceases when the density reaches integer values, i. e. for $\rho = 2$ and $\rho = 3$ we observe a plateau. Note that the second plateau is

larger than the first, which reflects the major localization of the particles for this filling, a fact that was previously reported for spinless bosons with three-body interaction terms.

An important fact is that the compressibility $\kappa = \partial\rho/\partial\mu$ is positive (see Fig. 2a). An opposite result means that the transitions are of the first order kind, which was stated for two-dimensional systems by Batrouni *et al.* [40] and de Forges de Parney [19] for spinless and spin-1 bosons, respectively. But for a spinor boson chain with two-body interactions, it was shown that transitions for even Mott lobes are of the first order, despite the fact that the compressibility is positive, indicating that the compressibility criterion is not sufficient to determine the type of transition [14]. Taking into account the above, we calculate the spin population fractions $N_+/N = N_-/N$ and N_0/N as a function of the global density (Fig. 2b). There are two different regions in this figure; for $\rho \leq 2$, the dominant projection is $\sigma = 0$ and $N_0/N \gg N_+/N$. This implies that ground state for $\rho = 2$ is not composed of singlets, because if so we would have to obtain that $N_+/N = N_-/N = N_0/N$, and this clearly does not happen. In the inset of Fig. 2a, we show that the square of the local moment ($\langle S^2 \rangle$) as a function of the hopping parameter t/V_0 for a fixed global density $\rho = 2$ remains around the same value $\langle S^2 \rangle \sim 3.2$ as the hopping increases from zero. This means that inside of the Mott insulator region (left of the vertical dashed line) $\langle S^2 \rangle$ is finite and non-zero, which means that the ground state is not composed of singlets, because if so, $\langle S^2 \rangle \rightarrow 0$ as t/V_0 goes to zero.

Based on Fig. 2b, we see that inside of the superfluid region, the global density drives a change in the ground state of the system, i. e. a quantum phase transition takes place around $\rho \approx 2.2$, and the system passes from a state where $N_0/N \gg N_+/N$ to a state with $N_+/N > N_0/N$, a fact that is a consequence of spin-dependent three-body interactions. Also, we observe in Fig. 2b that around integer densities the ground state is the same, which indicates that the quantum phase transitions will be of the first order for both even and odd Mott lobes. This result diverges from the two-body findings, where for even and odd Mott lobes first and second order transitions were found, respectively [14].

Knowing that the ground state of our system can be gapped or gapless, we can use this fact to draw a phase diagram, which is shown in Fig. 3 for the first two Mott lobes ($\rho = 2$ and $\rho = 3$) in the $(\mu/V_0, t/V_0)$ plane, for different values of spin dependent interaction V_2 . We observe that the Mott lobes are surrounded by a superfluid phase, similar to the spinor case with two-body interactions [11]. In Fig. 3a, we note that the phase diagram for $V_2/V_0 = 0$ coincides with the phase diagram predicted and reported for the spinless case with three-body interactions [30, 31]. Now the spin-dependent interaction is turned on, and we show in Fig. 3b and Fig. 3c that the Mott lobes are suppressed as the spin-dependent interaction parameter increases, implying that the position of

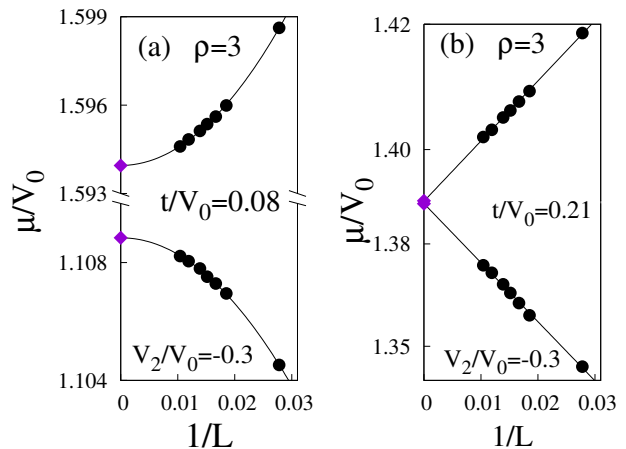


FIG. 5. Chemical potential as a function of the inverse of the lattice size for $\rho = 3$ and $V_2/V_0 = -0.3$. The left panel shows a state with a finite gap for $t/V_0 = 0.08$. The right panel shows a gapless behavior for $t/V_0 = 0.21$. The values at the thermodynamic limit (diamonds) were obtained by fitting the DMRG results (circles) in the left (right) panel to the function $\mu^{p,h}(L) = \tilde{\mu}^{p,h} + c_1/L + c_2/L^2$ ($\mu^{p,h}(L) = \tilde{\mu}^{p,h} + c_3/L$), where c_i are constants. The lines are visual guides.

the critical point moves to the left (small values of t/V_0). This behavior contrasts with the results for the two-body case, where the even Mott lobes grow while the odd ones decrease, exhibiting an even-odd asymmetry. Note that in Fig. 3 the numerical results at $t = 0$ are in accord with the atomic limit results.

According to several authors, for the spin-1 Bose-Hubbard model with two-body interactions, the Mott lobes exhibit interesting magnetic properties: some of these lobes can be in a dimerized, singlet, or nematic phase. For instance, in order to observe the dimerization, the spin-spin correlation function, the dimer susceptibility, or the dimer order parameter has been calculated in various studies [11, 12, 41]. In Fig. 4a, we show the spin-spin correlation function between neighboring sites for the second Mott insulator lobe ($\rho = 3$), and the parameters considered are $L = 32$, $t/V_0 = 0.05$, and $V_2/V_0 = 0.2$. Disregarding the border effects due to the open boundary conditions, we observe that spin-spin correlations between neighboring sites are ferromagnetic and exhibit an oscillating behavior around two values, which reflects the fact that there is a unit cell composed of two sites that repeats on the lattice; hence the odd Mott lobes have a dimer magnetic order, in a manner similar to the model with two-body interactions [11, 12, 16, 17]. In Fig. 4b, we present a possible dimerized configuration following F. Zhou's illustrations [42]. Here, the wells represent lattice sites, the balls represent the atoms, and three bosons per site were considered. Each boson has three spin orientations, of which we only show two (blue and red balls). Each pair of blue and red balls forms a singlet, and we can see a possible way in which the translational symmetry is broken. The dashed lines explicitly show the singlets

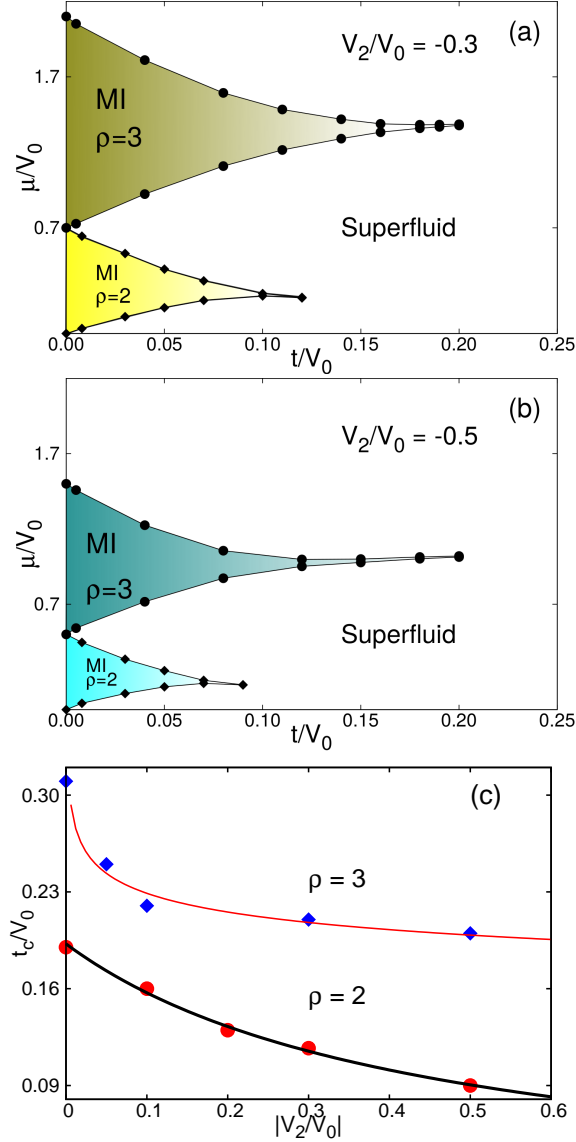


FIG. 6. Phase diagram for the first two Mott lobes of the $S = 1$ Bose-Hubbard model with three-body interaction and ferromagnetic spin interaction. The panels correspond to different values of $V_2/V_0 = -0.3$ (a) and $V_2/V_0 = -0.5$ (b). The solid lines are visual guides. (c) Evolution of the critical points with the spin exchange interaction parameter $|V_2/V_0|$. The solid lines correspond to the fit to the expressions (2) and (3) for the lobes $\rho = 2$ and $\rho = 3$, respectively.

that can form along the lattice, and we can observe that an alternating atom-atom correlation or singlet-singlet correlation between neighboring sites can happen, which explains the spin correlation function obtained in Fig. 4a.

B. Ferromagnetic case ($V_2 < 0$)

Now we consider a lattice of spin-1 atoms with a ferromagnetic local spin-dependent interaction. At the atomic limit, we expected that the border among the Mott lobes would depend on the spin-dependent strength, and to find the precise dependence, we have to take into account that the local spin must be at a maximum; hence $\langle \hat{S}_i^2 \rangle = n_i(n_i + 1)$ for all Mott lobes, where n_i is the number of atoms per site. Considering the above fact, the ground-state energy with n_i particles is $E_M(n_i) = \frac{V_0 + V_2}{6} n_i(n_i - 1)(n_i - 2)$. Therefore, the border between Mott lobes with n_i and $n_i + 1$ particles is given by $\mu_0(n_i \rightarrow n_i + 1) = \frac{V_0 + V_2}{2} n_i(n_i - 1)$. Then the upper border of the Mott insulator lobes depends on the local spin-dependent interaction, and we obtain $\mu_0^*/V_0 = 1 + \frac{V_2}{V_0}$ and $\mu_0^*/V_0 = 3 + 3\frac{V_2}{V_0}$ for the first and the second Mott lobe, respectively. Note that the above atomic limit expressions are in accordance with the numerical results shown in Figs. 6a and 6b.

In Fig. 5, we show the evolution of the chemical potential with the lattice size, fixing the global density at $\rho = 3$ and $V_2/V_0 = -0.3$. If we consider the kinetic energy parameter to be less than the repulsion interaction ($t/V_0 = 0.08$), we expect that at the thermodynamic limit, the chemical potential to increase or decrease the number of particles in one will tend to different values, and so a finite energy gap of $\Delta/V_0 \approx 0.485$ will be obtained (see Fig. 5a). Note that the above gapped state is obtained for an integer density and is due to the interaction between the atoms; therefore this is a Mott insulator state, for which we also observe that the energy for adding (removing) a particle decreases (increases) following a quadratic behavior, regardless of the sign of the local spin-dependent interaction. The increase of the kinetic energy ($t/V_0 = 0.21$) leads to more quantum fluctuations. The atoms tend to delocalize throughout the lattice, and the energy for adding or removing a particle follows a linear behavior with the inverse of the system size, reaching the same value at the thermodynamic limit. Therefore, for these parameter values the ground state is gapless and corresponds to a superfluid state (see Fig. 5b).

The phase diagram of spin-1 bosons with ferromagnetic local spin-dependent interaction in the plane $(\mu/V_0, t/V_0)$ is shown Fig. 6. It is composed of a superfluid phase that surround the Mott insulator lobes, which decrease when the absolute value of the three-body spin-dependent strength increases. In Fig. 6a and Fig. 6b, we observe that for a fixed number of bosons, the critical point that separates the Mott insulator and the superfluid regions evolves in a different way, depending on the global density: the first (second) Mott lobe decreases quickly (slowly). Using the vanishing gap criteria, we estimate the position of the critical point for each value of V_2 and obtain the points of Fig. 6c, where it is possible to see the differing behavior of the critical points of the first and second Mott lobes. The lower solid line shown in this fig-

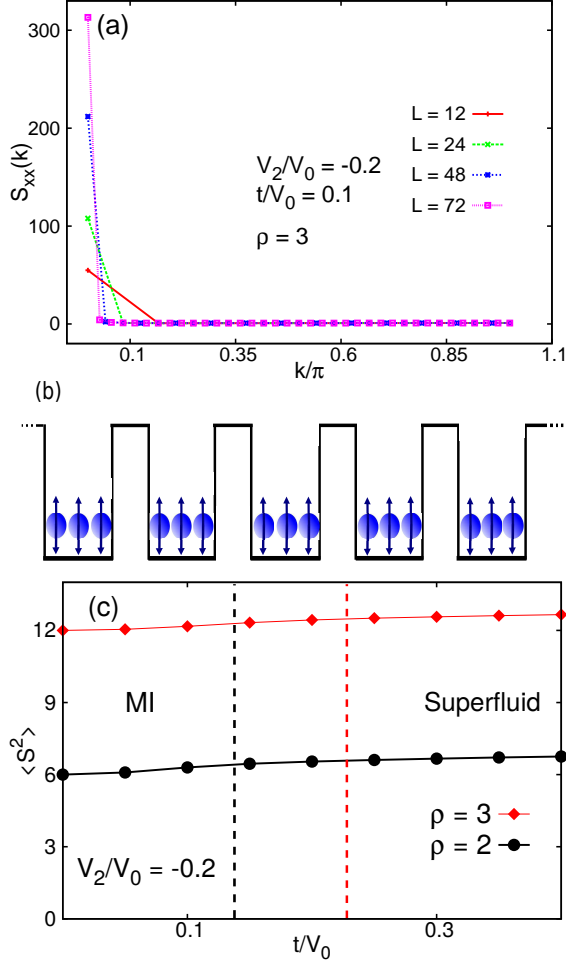


FIG. 7. (a) The x -axis spin structure factor $S_{xx}(k)$ for a spinor boson chain with ferromagnetic spin-dependent interaction inside of the second Mott lobe ($\rho = 3$). Here $V_2/V_0 = -0.2$ and $t/V_0 = 0.1$. (b) Schematic of a microscopic configuration for “long-range” ferromagnetic order. (c) The expectation value $\langle \hat{S}_i^2 \rangle$ as a function of the hopping t/V_0 for the two first lobes with $V_2/V_0 = -0.2$.

ure is the adjusted fit for $\rho = 2$ using the expression

$$\frac{t_c}{V_0} = \frac{1}{a \frac{V_2}{V_0} + b}, \quad (2)$$

where $a = 11.63 \pm 0.51$ and $b = 5.20 \pm 0.17$ are constants, while for $\rho = 3$, we describe the evolution of the critical point following the expression

$$\frac{t_c}{V_0} = \alpha \left(\frac{V_2}{V_0} \right)^\beta + \gamma, \quad (3)$$

where the constants take the following values: $\alpha = 0.115 \pm 0.081$, $\beta = 0.166 \pm 0.071$, and $\gamma = 0.304 \pm 0.035$.

Also, in the second Mott lobe it is possible to observe a reentrant behavior; however, we believe that this is due to the truncation of the local Hilbert space, and therefore

if we increase the number of possible states in the local Hilbert space, this may not be observed.

In order to determine the magnetic order and to determine how the local moments are oriented from site to site, we calculated the spin structure factor by means of the correlation functions given by

$$S_{\sigma\sigma}(k) = \sum_{\ell} e^{ik\ell} \langle S_{\sigma,j+\ell} S_{\sigma,j} \rangle, \quad (4)$$

where σ can be x or z .

In Fig. 7a, we show $S_{xx}(k)$ in the Mott insulator state at $t/V_0 = 0.1$. We consider three atoms per lattice site and ferromagnetic interaction $V_2/V_0 = -0.2$. We obtain a peak at $k = 0$, indicating that the Mott phase has a ferromagnetic order. We can see that this peak grows with the lattice size, showing a “long-range” ferromagnetic order. A schematic of the microscopic configuration of the atoms is shown in Fig. 7b, where it is possible to observe all the local moments in the same direction (we chose the “up” direction to illustrate the behavior). During the discussion of the atomic limit, we said that to consider a ferromagnetic interaction leads to the expectation value $\langle \hat{S}_i^2 \rangle$ being a maximum. This is shown in Fig. 7c, where we calculate the value of $\langle S_i^2 \rangle$ as a function of t/V_0 and observe that this quantity remains constant for $\rho = 2$ and 3. Note that the numerical value corresponds to $\langle S_i^2 \rangle = n_i(n_i + 1) \approx 6$ and 12, respectively. Also, we calculate the magnetic structure factor in the superfluid phase, and it is also ferromagnetic.

IV. CONCLUSIONS

In this paper, we studied the ground state of spin-1 bosons loaded in a one-dimensional optical lattice, using the $S = 1$ Bose-Hubbard model with local three-body interaction terms at zero temperature. In order to determine the phase diagram, we employed the density matrix renormalization group method with a maximum of five bosons per site, and we obtained that the ground state of the model exhibits a superfluid or a Mott insulator state, regardless of the sign of the local spin-dependent interaction. The Mott insulator region with one boson per site is absent in the phase diagrams, while for larger densities the Mott lobes increase with the density, reflecting a higher localization in the system. We show that at the atomic limit the borders between different Mott lobes always depend on the local three-body spin-dependent interaction, a fact that leads to the Mott insulator regions always decrease as the spin-dependent strength parameter increases for both ferromagnetic and antiferromagnetic interaction. The above statement contains an important result, which is that for antiferromagnetic interaction, a one-dimensional system of spin-1 bosons that interact under local three-body interactions, the even-odd asymmetry is absent, which differs from the two-body case, where this asymmetry is the most relevant result, remarked by several authors.

For antiferromagnetic spin-dependent interaction, we observe that the odd lobes are dimerized, while the even lobes are not composed of singlets. When the global density increases while the other system parameters are fixed, the spinor chain passes from a superfluid to a Mott insulator state for densities larger than one. These quantum phase transitions are of the first-order kind for both even and odd lobes. Also, the spin-dependent interaction generates a quantum phase transition inside of the superfluid region for a density $\rho \approx 2.2$, regardless of the hopping parameter value.

For ferromagnetic coupling, both the Mott insulator and the superfluid phase exhibit a “long-range” ferro-

magnetic order, and we found that the critical points move to lower values as the spin interaction increases, and their evolution depends on the global density.

ACKNOWLEDGMENTS

The authors are thankful for the support of DIEB- Universidad Nacional de Colombia and Departamento Administrativo de Ciencia, Tecnología e Innovación (COL-CIENCIAS) (grant No. FP44842-057-2015). J.S.-V. and R.F. are grateful for the hospitality of the ICTP, where part of this work was done.

-
- [1] B. P. Anderson and M. A. Kasevich, *Science* **282**, 1686 (1998).
 - [2] M. Greiner *et al.*, *Nature* **415**, 39 (2002).
 - [3] D. Jaksch, C. Bruder, J. Cirac, C. Gardiner, and P. Zoller, *Phys. Rev. Lett.* **81**, 3108 (1998).
 - [4] T. D. Kühner and H. Monien, *Phys. Rev. B* **58**, 14741(R) (1998).
 - [5] T. D. Kühner, S. R. White, and H. Monien, *Phys. Rev. B* **61**, 12474 (2000).
 - [6] S. Ejima, H. Fehske, and F. Gebhard, *Europhys. Lett.* **93**, 30002 (2011).
 - [7] D. M. Stamper-Kurn, M. R. Andrews, A. P. Chikkatur, S. Inouye, H.-J. Miesner, J. Stenger, and W. Ketterle, *Phys. Rev. Lett.* **80**, 2027 (1998).
 - [8] E. Demler and F. Zhou, *Phys. Rev. Lett.* **88**, 163001 (2002).
 - [9] A. Imambekov, M. Lukin, and E. Demler, *Phys. Rev. A* **68**, 063602 (2003).
 - [10] S. Tsuchiya, S. Kurihara, and T. Kimura, *Phys. Rev. A* **70**, 043628 (2004).
 - [11] M. Rizzi, D. Rossini, G. D. Chiara, S. Montangero, and R. Fazio, *Phys. Rev. Lett.* **95**, 240404 (2005).
 - [12] V. Apaja and O. F. Syljuasen, *Phys. Rev. A* **74**, 035601 (2006).
 - [13] R. V. Pai, K. Sheshadri, and R. Pandit, *Phys. Rev. B* **77**, 014503 (2008).
 - [14] G. G. Batrouni, V. G. Rousseau, and R. T. Scalettar, *Phys. Rev. Lett.* **102**, 140402 (2009).
 - [15] S. S. Natu, J. H. Pixley, and S. D. Samara, *Phys. Rev. B* **91**, 043620 (2015).
 - [16] S. K. Yip, *Phys. Rev. Lett.* **90**, 250402 (2003).
 - [17] S. Bergkvist, I. P. McCulloch, and A. Rosengern, *Phys. Rev. A* **74**, 053419 (2006).
 - [18] Y. Toga, H. Tsuchiura, M. Yamashita, K. Inaba, and H. Yokoyama, *J. Phys. Soc. Jpn.* **81**, 063001 (2012).
 - [19] L. de Forges de Parny, F. Herbert, V. G. Rousseau, and G. G. Batrouni, *Phys. Rev. B* **88**, 104509 (2013).
 - [20] L. de Forges de Parny, H. Yang, and F. Mila, *Phys. Rev. Lett.* **113**, 200402 (2014).
 - [21] K. W. Mahmud and E. Tiesinga, *Phys. Rev. A* **88**, 023602 (2013).
 - [22] H. Büchler, A. Micheli, and P. Zoller, *Nat. Phys.* **3**, 726 (2007).
 - [23] P. R. Jhonson, E. Tiesinga, J. V. Porto, and C. J. Williams, *New J. Phys.* **11**, 093022 (2009).
 - [24] S. Will, T. Best, U. Schneider, L. Hackermüller, D.-S. Lühmann, and I. Bloch, *Nature* **465**, 197 (2010).
 - [25] R. Ma, M. E. Tai, P. M. Preiss, W. S. Bakr, J. Simon, and M. Greiner, *Phys. Rev. Lett.* **107**, 095301 (2011).
 - [26] S. Paul and E. Tiesinga, *Phys. Rev. A* **92**, 023602 (2015).
 - [27] A. J. Daley and J. Simon, *Phys. Rev. A* **89**, 053619 (2014).
 - [28] S. Paul, P. . R. Johnson, and E. Tiesinga, *Phys. Rev. A* **93**, 043616 (2016).
 - [29] B.-L. Chen, X.-B. Huang, S.-P. Kou, and Y. Zhang, *Phys. Rev. A* **78**, 043603 (2008).
 - [30] J. Silva-Valencia and A. M. C. Souza, *Eur. Phys. J. B* **85**, 161 (2012).
 - [31] T. Sowiński, *Phys. Rev. A* **85**, 065601 (2012).
 - [32] V. K. Varma and H. Monien, *Phys. Rev. B* **90**, 085138 (2014).
 - [33] B. Capogrosso-Sansone, S. Wessel, H. Büchler, P. Zoller, and G. Pupillo, *Phys. Rev. B* **79**, 020503(R) (2009).
 - [34] A. Safavi-Naini, J. von Stecher, B. Capogrosso-Sansone, and S. T. Rittenhouse, *Phys. Rev. Lett.* **109**, 135302 (2012).
 - [35] D. M. Stamper-Kurn and M. Ueda, *Rev. Mod. Phys.* **85**, 1192 (2013).
 - [36] T. L. Ho, *Phys. Rev. Lett.* **81**, 742 (1998).
 - [37] T. Ohmi and K. Machida, *J. Phys. Soc. Jpn.* **67**, 1822 (1998).
 - [38] S. R. White, *Phys. Rev. Lett.* **69**, 2863 (1992).
 - [39] H. Katsura and H. Tasaki, *Phys. Rev. Lett.* **110**, 130405 (2013).
 - [40] G. G. Batrouni, and R. T. Scalettar, *Phys. Rev. Lett.* **84**, 1599 (2000).
 - [41] P. Chen, Z. L. Xue, I. P. McCulloch, M. C. Chung, and S. K. Yip, *Phys. Rev. A* **85**, 011601(R) (2012).
 - [42] F. Zhou, *Europhys. Lett.* **10**, 1209 (2003).

